

## CORRELATION BETWEEN MICRO-STRUCTURE AND ACOUSTIC EMISSION CHARACTERISTICS OF GRANITE BY SPLIT TESTS

by

**Qian-Cheng GENG<sup>a,b</sup>, Shuang YOU<sup>a,b\*</sup>, Huan WANG<sup>a,b</sup>,  
Hong-Guang JI<sup>a,b</sup>, Xiu-Feng ZHANG<sup>c</sup>, and Yang CHEN<sup>c</sup>**

<sup>a</sup>Beijing Key Laboratory of Urban Underground Space Engineering, USTB, Beijing, China  
<sup>b</sup>School of Civil and Resources Engineering, University of Science and Technology Beijing,  
Beijing, China

<sup>c</sup>Shandong Energy Group Co., LTD, Jinan Shandong, China

Original scientific paper  
<https://doi.org/10.2298/TSCI2301663G>

*The mesoscopic structure of rocks determines their strength and deformation characteristics. The grain and pore size distribution of granite samples buried depth of 1600 m to 1900 m in a goldmine of Shandong Province are measured by polarizing microscope and low-field nuclear magnetic resonance. The splitting test is carried out and the acoustic emission signal is obtained in real time by using an electro-hydraulic servo press and PCI-2 acoustic emission collector. The relationship between meso-mechanics and acoustic emission characteristics of split granite is analyzed. The experimental result shows that there is no clear correlation between meso-grain size and pore size distribution. Rocks with larger mineral grains easily form inter-embedded structures between grains and grains, the bearing effect of grains is enhanced, and the tensile strength of rocks is improved. The level of stress concentration in the rock is closely related to the pore size of the rock, and the acoustic emission ringing count before the main rupture in the large aperture (0.1~10 μm) of the rock is more active than that of the small aperture rock (0.01~1 μm), and a large number of high frequency acoustic signals are induced by the penetration between the pores in the unstable failure stage and post-peak failure stage, the stress concentration is higher, and the energy release frequency is increased, however the energy released strength by a fracture is weak.*

Key words: deep granite, splitting test, acoustic emission, micro-structure

### Introduction

Differences in the meso-structure of rocks affect their strength and deformation characteristics [1]. The experimental study on the relationship between rock meso-structure and macroscopic mechanical properties can not only reveal the substantial mechanism of the different macroscopic properties of rock, but also improve the bridge between meso-mechanics and macro-mechanics [2]. Acoustic emission (AE) signals can directly show the activity of crack development and expansion. At present, AE technique is still one of the ef-

---

\*Corresponding author, e-mail: youshuang@ustb.edu.cn

fective means to monitor the microstructure evolution of rock [3]. This paper will focus on the macroscopic mechanical properties and the evolution of AE signals when there are differences in the meso-structure of granite.

The macroscopic mechanical properties of rock depend on its mineral composition and meso-structure. Fu *et al.* [4] studied the effect of random mesoscopic structure on the macroscopic mechanical behavior of rocks based on MFPA, revealing the influence of random mesoscopic structure on the failure process of brittle materials. Wu *et al.* [5] explored the micro-failure process and failure mechanism of a typical brittle rock under uniaxial compression, which are investigated via continuous real-time measurement of wave velocities.

The differences in rock meso-structure should be reflected in the characteristics of AE [6]. Based on micro- and macro-crack damage of rock, Moradian *et al.* [7] divided the crack levels into eight stages by AE signal parameter analysis. Current experiments show that the influence of rock meso-structure differences on the micro-crack propagation mode is indeed reflected in the AE characteristics of rocks [8]. However, there are few studies on the difference of meso-structure in AE characteristics, and the mechanism of meso-structure on rock mechanical properties is not clear.

The grain and pore size distribution of granite buried in the depth of 1600 m to 1900 m in a goldmine of Shandong Province were measured by polarizing microscope and low-field nuclear magnetic resonance (NMR). The splitting test is carried out and AE signal is acquired during the test by the time. The meso-structure changes on the mechanical and AE character of split granite are measured and analyzed.

### Test samples and test methods

Rock samples were taken from the cores of the geology exploration holes in a goldmine of Shandong Province. Those cores were made into a disk sample with a diameter of 50 mm and a thickness of 25 mm for splitting tests. The parameters are shown in tab. 1.

**Table 1. Testing sample**

Rock type	Depth, [m]	Average tensile strength, [MPa]	Density, [kgm <sup>-3</sup> ]	Ultrasonic speed, [ms <sup>-1</sup> ]
Granite	1600	8.91	2618	2604
Granite	1700	9.56	2635	3289
Granite	1800	8.42	2619	3125
Granite	1900	7.75	2597	2606

Firstly, the samples at different depths were prepared into micro-slices, and the mineral composition, morphology and particles were observed by polarized light microscope. Then, the rocks were vacuum-saturated, and the distribution characteristics of water molecules in pores of different sizes inside the rocks were detected by NMR to obtain the T2 spectrum distribution. The ZYB-II type vacuum pressure saturation device was adopted in the process of water saturation. The vacuum pump rate was 2 Lpm, the vacuum degree was -0.1MPa, and the water retention time was 12 hours. The low-field NMR experiment was performed using a Meso MR23-060H-I NMR instrument at a resonance frequency of 23 MHz. Finally, according to the relationship between T2 relaxation time and core pore radius, the pore size distribution characteristics of the rock could be obtained.

After the meso-structure tests, the splitting mechanics tests were carried out, and the AE signals were collected during the test. The splitting loading testing machine is a micro-computer-controlled electro-hydraulic servo universal machine. The loading mode is load control, and the loading rate is 60 N/s. The acoustic signal acquisition device is a PCI-2 AE

acquisition collector, using two probes with resonant frequencies of 60 kHz low frequency and 150 kHz high frequency respectively, and the threshold value of AE acquisition is 45 dB. During the test, the sample was preloaded with 1kN to stabilize the sample, and then the press, AE acquisition collector and strain acquisition collector were started at the same time. After the rock was split into two parts, each acquisition device was stopped and the data was saved.

### Rock meso-structural characteristics and splitting mechanical characteristics

According to the polarizing microscope test, the rock mineral composition of each depth is basically the same which the main minerals potassium feldspar, plagioclase and quartz account for more than 90%. The rocks at the 1700 m depth contain small amounts of white mica and calcite, while other deeper rocks contain small amounts of black mica and chlorite. The rock samples with burial depths of 1600 m and 1700 m are medium and coarse-grained granite structures, and the rock samples with burial depths of 1800 m and 1900 m are medium-grained granite structures.

Figure 1 shows the pore size distribution characteristics of rocks at various depths detected by low-field NMR experiment. It can be seen from fig. 1 that the pore size of the rock samples with a buried depth of 1600 m and 1800 m is mainly concentrated between 0.1 and 10  $\mu\text{m}$ , the pore size of the rock samples with a buried depth of 1700 m is mainly concentrated between 0.01  $\mu\text{m}$  and 1  $\mu\text{m}$ , and the pore size of the rock samples with a buried depth of 1900 m is between the two types of rocks.

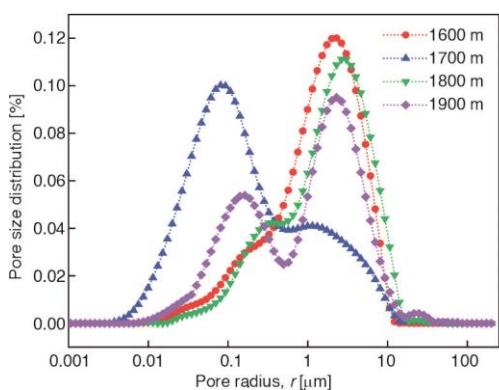


Figure 1. Pore size distribution

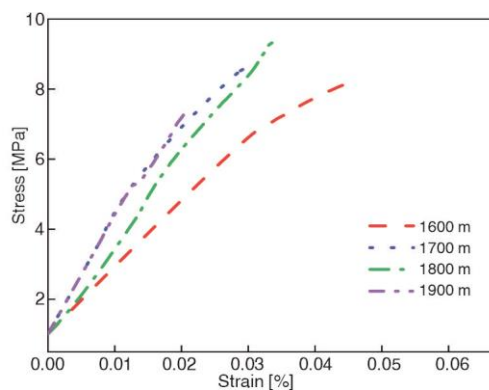


Figure 2. Splitting stress-strain curve

In order to better describe the pore size, the classification proposed by Yu *et al.* [9] was integrated, and the pore size of 0.1~10  $\mu\text{m}$  was considered as large apertures, and the pore size of 0.01~1  $\mu\text{m}$  was considered as small apertures. According to the microscopic test results and NMR, the rock samples at 1600 m and 1700 m are medium-coarse rocks, but the mesoscopic pore sizes at 1600 m are dominated by larger sizes, and the mesoscopic pore sizes at 1700 m are dominated by small sizes. The rock samples with the burial depth of 1800 m and 1900 m are medium-grained structure, but the mesoscopic pore size of 1800 m is a mainly large size, and the mesoscopic pore size of 1900 m is distributed between large size and small size. The integration results of meso-structural characteristics of granite samples at various depths are shown in tab. 2.

The experimental results show that there is no clear correlation between meso-grain size and pore size distribution. The size of rock crystals only affects the intergranular pore size distribution characteristics, while the actual pore size distribution characteristics by the intragranular cracks and intergranular cracks of rock weave together while the actual pore size distribution characteristics by the rock intracrystalline fractures and intergranular fractures together weave.

**Table 2. Characteristics of granite particle size and pore size**


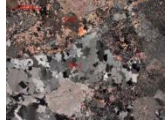
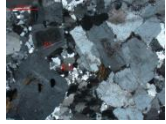
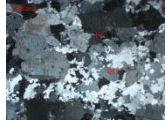
Depth, [m]	Particle size	Pore size	Image
1600	1.2~7.5 mm Medium-coarse-grained	0.1~10 $\mu\text{m}$	
1700	1~7 mm Medium-coarse-grained	0.01~1 $\mu\text{m}$	
1800	0.8~5.5 mm Medium-grained	0.1~10 $\mu\text{m}$	
1900	0.9~5.2 mm Medium-grained	0.01~10 $\mu\text{m}$	

Figure 2 indicates the stress-strain curve diagram of splitting granite at various depths. Medium coarse granites buried at depths of 1600 m and 1700 m showed ductility characteristics when close to tensile strength, while medium-grain granites buried at depths of 1800 m and 1900 m showed brittle cracking characteristics. In addition, the average tensile strength of the tested medium-coarse-grained granite is slightly higher than that of the medium-grained granite. The structure shows that in granite with larger grains, small grains are more easily embedded between large grains, and more intercalation structures are formed between grains, the high strength of the mineral composition gives more play to its bearing capacity. In the spatial strength distribution of rocks, there is a strong heterogeneity, and the inhomogeneous spatial distribution of mineral components makes it easy to have local micro-ruptures during rock loading, and the stiffness of rocks is gradually reduced, showing good ductility characteristics.

According to the tensile stiffness values, the rock stiffness buried at a depth of 1700 m is significantly higher than the rocks at other depths. The deformation of rocks is mainly due to the closing and stretching action of cracks. It can be seen from the microscopic pore distribution characteristics that the granite buried depth of 1700 m is mainly small pores, so it is not easy to deform under low stress level, so the stiffness is large. The granite with a burial depth of 1900 m has a slightly higher stiffness than the other three groups due to the higher proportion of small and medium-sized pores. When the difference in porosity between rocks is not large, the smaller the average pore size, the smaller the deformation capacity of the rock, so its stiffness value will be larger.

## Acoustic emission characteristics of splitting tests

### *Cumulative ringing count of Acoustic emission*

The AE is the stress wave released by the expansion of micro-cracks in the rock. The AE ringing count can reflect the active degree of micro-crack propagation in the rock. As shown in fig. 3, the loading process of each group of rocks was normalized, and the tensile strength was divided into 10 equal parts to calculate the variation trend of the cumulative ringing count under each stress level. It can be seen from Figure. 3 that the cumulative ringing counts of the granites with buried depths of 1600 m, and 1800 m in each stress stage are significantly higher than those of the other two groups. From the distribution characteristics of mesoscopic pore size, it can be seen that the granite with buried depths of 1600 m, and 1800 m are mainly large apertures, and large apertures are more likely to expand under low-stress levels and release more AE signals. The granite with a buried depth of 1700 m and 1900 m contains more small apertures, which are difficult to expand under low-stress levels, so the acoustic signal is not active at low-stress levels.

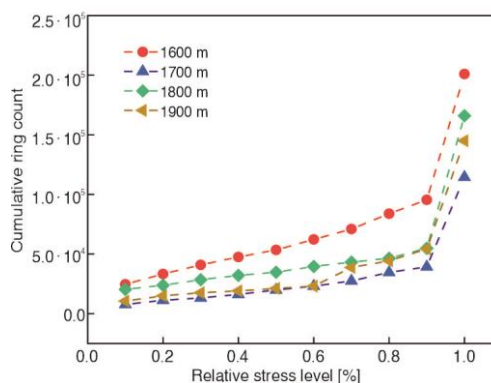


Figure 3. The AE cumulative ringing count of different buried depths

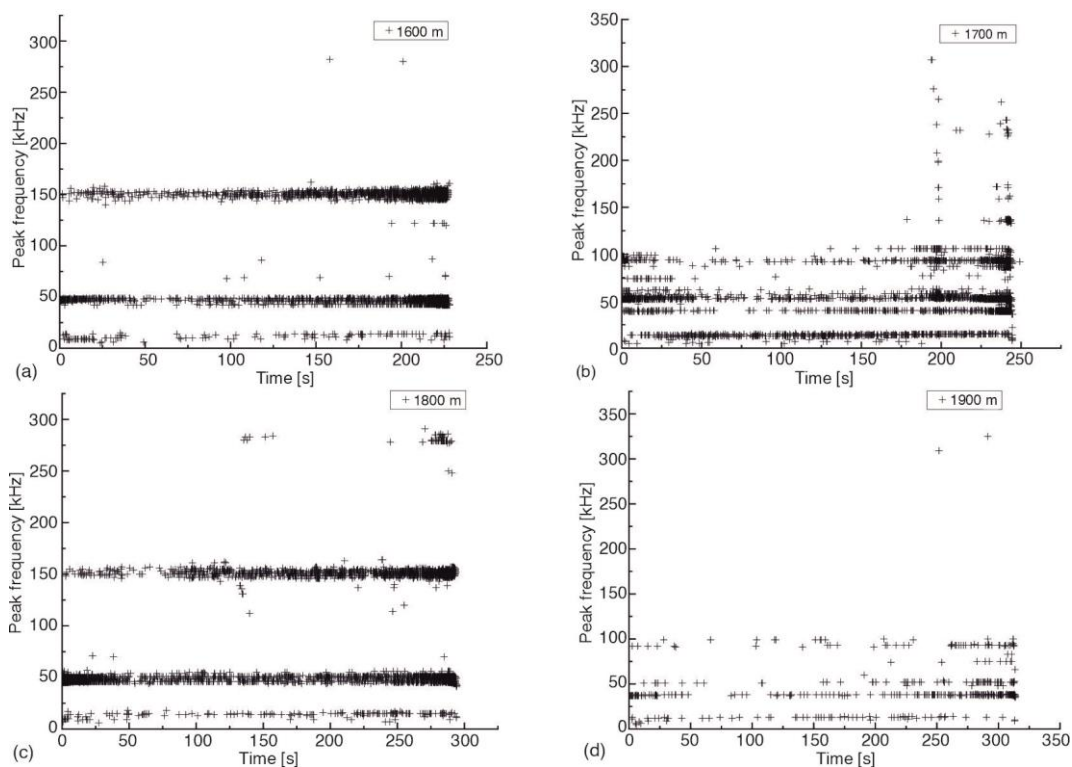
### *Distribution characteristics of acoustic emission peak frequency*

The simple harmonic vibration corresponding to the peak frequency of AE can be close to the frequency characteristics of the actual acoustic signal to the maximum extent [10]. The higher the frequency of acoustic signal is, the greater the restoring force of the fractured vibration region inside the rock.

By analyzing the full waveform of AE and the evolution law of primary and secondary frequencies, the acoustic signals from 0 kHz to 100 kHz are regarded as low frequency signals, the acoustic signals from 100 kHz to 200 kHz are regarded as medium frequency signals, while those above 200 kHz are regarded as high frequency signals, revealing the rupture destabilization process of rocks. It can be seen from the characteristic diagram of a peak frequency distribution of AE in fig. 4 that in the early stage of the loading process of samples buried at 1600 m, and 1800 m, the acoustic signals are mainly medium and low frequency signals, and the signal points in each frequency band are densely distributed. In the un-stable failure stage and post peak failure stage, high-frequency signals with a peak frequency above 200 kHz appeared in large quantities. The granite buried at a depth of 1700 m has the absence of medium and low frequency bands and sparse distribution of frequency points in the linear elastic loading stage. The granite with a buried depth of 1900 m is sparsely distributed in the low frequency signal points in linear elastic loading stage, and there is no obvious medium and high frequency signal in the rock during the whole loading process.

Combined with the meso-structure characteristics of rock, it can be seen that the granite with the buried depth of 1600 m and 1800 m mainly has large apertures, and the cracks are more likely to expand, so the frequency points of each frequency band are densely distributed in the early stage of the loading process. The large apertures distribution in the rock makes it easy produce stress concentration between the pores, especially with the in-

crease of stress level, the large apertures gradually expand and penetrate in the middle and later stages of loading, which induces the generation of high-frequency signals. The granite buried at a depth of 1700 m mainly has small apertures, which are not easy to be broken under low stress level. Therefore, the frequency distribution of each frequency band is sparse in the early stage of the loading process, and even the frequency band is missing. The small size of the aperture improves the co-ordination of rock deformation, and local crack penetration rarely occurs in the middle of loading process. Thus, there is almost no high frequency signal before splitting, and the small-size pore crack penetrates to form a large aperture channel in the later loading stage, inducing a small amount of medium and high frequency signal generation. The granite buried at a depth of 1900m contains both large and small apertures. A considerable number of small apertures make the frequency distribution of the rock at this depth sparse, while the large aperture makes the rock not appear with high-frequency acoustic signals until the moment of failure.



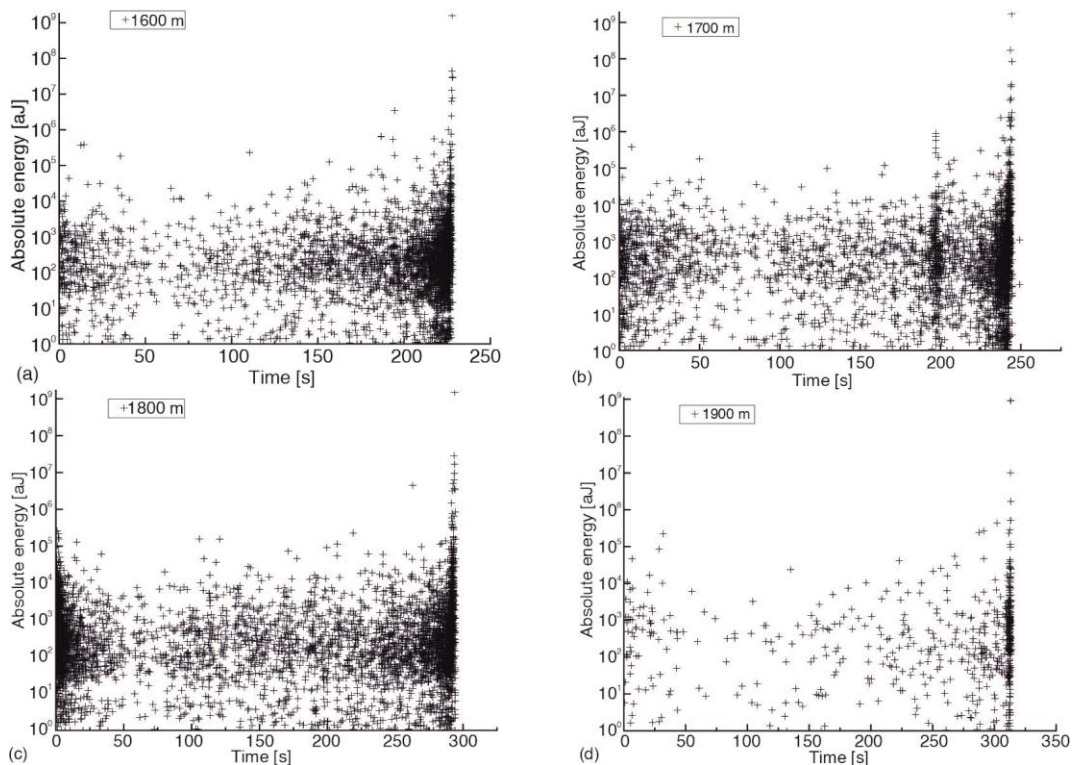
**Figure 4.** Characteristic diagram of peak frequency distribution of AE; (a) 1600 m, (b) 1700 m, (c) 1800 m, and (d) 1900 m

#### *Acoustic emission energy distribution*

Figure 5 shows the change of granite AE energy with time from 1600 m depth to 1900 m depth. Combined with figs. 1 and 5, it can be seen that for the granite at 1600 m and 1800 m depth has more large apertures, and the energy release is concentrated in the fracture closure stage, instability stage and post-peak damage stage, and the energy release is more sparse in the elastic loading stage. Granite at 1700 m and 1900 m depth has more small size pores, and the energy release is shorter. The higher the proportion of large pore size pores in



the rock, the more the number of energy release and the more dispersed the energy distribution, which is due to the fact that large pore size pores close and release a lot of energy in the fracture closure stage, while small size pores are not easy to rupture in loading and release energy in the unstable stage and post-peak damage stage with concentrated rupture.



**Figure 5. Characteristic diagram of energy distribution of AE; (a) 1600 m, (b) 1700 m, (c) 1800 m, and (d) 1900 m**

## Conclusion

The grain size and pore size distribution characteristics of the granite samples were detected by polarizing microscope and NMR. There is no clear correlation between meso-grain size and pore size distribution for such granite. The meso-grain size mainly affects the strength and ductility of granite. The rocks with larger mineral grains are prone to form inter-embedded structure among grains, the high-strength mineral composition exerts a greater load-bearing capacity, and the tensile strength of the rock is increased. In addition, the inhomogeneous spatial strength distribution caused by the increase of particle size makes granite prone to induce micro-fissure evolution before the macroscopic fracture, and the rock stiffness gradually decreases, and presents ductile phenomenon. The distribution characteristics of meso-pore size affect the deformation stiffness of granite. Large pore rocks ( $0.1\sim 10\ \mu\text{m}$ ) have a small deformation stiffness compared to small pore rocks ( $0.01\sim 1\ \mu\text{m}$ ). The rock with large pore exhibits an effective energy dissipation structure to reduce the energy storage capacity of the rock. The effect of rock pore size on the degree of stress concentration is verified by the AE response characteristics. The AE response of rocks with large apertures is

characterized by active AE bell counts before the main fracture of the rock, and a large number of high-frequency acoustic signals are induced by the penetration between the pores in the unstable failure stage and post peak failure stage, and relatively dispersed during energy release, weak average energy at single rupture.

### Acknowledgment

This work was supported by the National Natural Science Foundation of China (Grant No. 52074021), the Key Research Development Program of Shandong Province (2019SDZY02, 2019SDZY05) and the Fundamental Research Funds for the Central University (FRF-GF-20-01B).

### References

- [1] Eberhardt, E., *et al.*, Effects of Grain Size on the Initiation and Propagation Thresholds of Stress-induced Brittle Fractures. *Rock Mechanics and Rock Engineering*, 32 (1999), 2, pp. 81-99
- [2] Zang, Z. Y., *et al.*, Indications of Risks in Geothermal Systems Caused by Changes in Pore Structure and Mechanical Properties of Granite: An Experimental Study, *Bulletin of Engineering Geology and the Environment*, 79 (2020), 10, pp. 5399-5414
- [3] Zang, Z. P., *et al.*, Differences in the Acoustic Emission Characteristics of Rock Salt Compared with Granite and Marble During the Damage Evolution Process, *Environmental Earth Sciences*, 73 (2015), 11, pp. 6987-6999
- [4] Fu, Y. F., *et al.*, Influence of Stochastic Mesoscopic Structure on Macroscopic Mechanical Behavior of Brittle Material, *Proceedings*, 4<sup>th</sup> International Conference on Fracture and Strength of Solids, Pohang, South Korea, 2000, Vol. 411, pp. 785-790
- [5] Wu, Z. J., *et al.*, Micro-failure Process and Failure Mechanism of Brittle Rock under Uniaxial Compression Using Continuous Real-time Wave Velocity Measurement, *Journal of Central South University*, 28 (2021), 2, pp. 556-571
- [6] Lockner, D., The Role of Acoustic Emission in the Study of Rock Fracture, *International Journal of Rock Mechanics and Mining Sciences & Geomechanics Abstracts*, 30 (1993), 7, pp. 883-899
- [7] Moradian, Z., *et al.*, Detection of Cracking Levels in Brittle Rocks by Parametric Analysis of the Acoustic Emission Signals, *Rock Mechanics and Rock Engineering*, 49 (2016), 3, pp. 785-800
- [8] Guo, Y. X., *et al.*, Stress-strain-acoustic Responses in Failure Process of Coal Rock with Different Height to Diameter Ratios under Uniaxial Compression, *Journal of Central South University*, 28 (2021), 6, pp. 1724-1736
- [9] Yu, S. T., *et al.*, A New Method for Characterizing the Pore Size Distribution of Rock by Combing Nuclear Magnetic Resonance and Multistage Centrifuge, *Arabian Journal for Science and Engineering*, 47 (2022), 9, pp. 12253-12264
- [10] Antonaci, P., *et al.*, Fatigue Crack Propagation Monitoring by Acoustic Emission Signal Analysis, *Proceedings*, 29<sup>th</sup> National Conference of the Italian-Association-for-Stress-Analysis, Maratea, Italy, 2012, Vol. 81, pp. 26-32